Applied Thermal Engineering 231 (2023) 120910

Contents lists available at ScienceDirect

Applied Thermal Engineering

journal homepage: www.elsevier.com/locate/ate

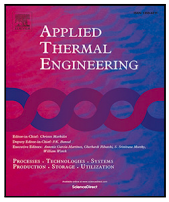

Research Paper

Adapted composite two-region line source methods for evaluation of borehole heat exchangers with advanced materials

Javier F. Urchueguía *, Borja Badenes, Hossein Javadi, Miguel Ángel Mateo, Bruno Armengot

ICT vs Climate Change research group - Instituto de Aplicaciones de las Comunicaciones Avanzadas (ITACA), Universitat Politècnica de València, Camino de Vera S/N, 46022 Valencia, Spain

ARTICLE INFO

Keywords:
Shallow geothermal energy
Thermal Response Test
Infinite line-source method
Two-region composite line-source method
Borehole resistance
Parameter estimation methods

ABSTRACT

The results of a large number of Thermal Response Tests (TRTs) performed on four different borehole heat exchangers (BHEs) were analyzed to explore the effect of the novel grouting and plastic pipe materials developed in a previous project on their thermal performance. For this purpose, two versions of the composite two-region line source approach have been adapted for its use for evaluating BHEs in practical situations, allowing us to obtain more comprehensive and consistent information on key thermal parameters of ground and fillers. We develop a scheme that combines the composite two-region model with unsteady TRT injection data to avoid some shortcomings that have appeared in previous implementations of this approach. Our new method enables us to obtain parameters otherwise difficult to obtain, such as the diffusivities, heat capacities, and conductivities of ground and grout. In comparison with standard line source based analysis, it allows to improve and enrich TRT execution, with a reduction in the test time required, lower uncertainties of the parameters obtained, and a deeper understanding of the thermal properties of the grout, ground, and borehole heat exchanger as all estimates are correlated to actual physical, mensurable soil and ground properties, which allows independent critical revision and check against alternative estimation methods.

1. Introduction

Shallow geothermal energy (SGE) is continuous, renewable and efficient source of thermal energy, with significant advantages for heating and cooling of buildings compared to other technologies, [1] such as high system performance due to the operating conditions of the SGE, resulting in considerable cost savings, free space on roofs and no visual impacts. However, given the higher upfront capital required compared to alternative options, particularly gas or other fossil technologies, the poor awareness, and the varied and shifting regulatory landscapes, its application on a broad scale poses a significant barrier. Therefore, many ongoing projects focusing on capital cost reduction, improved efficiency, increased reliability, and security are meant to overcome these difficulties. This includes research on novel materials [2–4], faster and cheaper drilling techniques [5], optimized geometries [6] and system-wide engineering advancements, as well as enhanced controls, amongst other topics [7].

In addition, the borehole heat exchangers (BHE) can be integrated into foundation components such as tunnel linings, piles or basement walls, employing energy geostructures. Energy geostructures serve the dual purpose of exchanging heat and load-bearing, allowing them to circulate a fluid of varying temperatures to transfer the energy from/to the ground. Adopting these geostructures to the GSHP systems, the initial installation costs can be decreased [8–10]

Regardless of the desired improvement, a fundamental requirement is to acquire adequate data to evaluate the performance that a particular solution can provide, as well as the potential cost increase. To achieve this, experimental methods to evaluate the performance of borehole heat exchangers (BHEs), such as Thermal Response Tests (TRTs), are crucial.

In-situ TRTs are used frequently to ascertain the thermal characteristics of the ground and BHEs to be installed in real-world applications (see [11–13] for a recent review). These thermal tests are based on comparing the measured BHE's temperature response to a continual heat injection, with the prediction of a given model based on a few fitting parameters, such as soil thermal conductivity.

To achieve proper analysis, the model used is essential [11]. The Kelvin line-source theory, commonly known as the infinite line-source (ILS) model, [11,12], is one of the earliest and most often used models (owing to its simplicity and speed, [14]). The cylinder-source (CLS), [15,16], and the finite line-source (FLS) approaches, [17–19],

* Corresponding author.
E-mail addresses: jfurchueguia@fis.upv.es (J.F. Urchueguía), borbaba@upv.es (B. Badenes), hjavadi@upv.es (H. Javadi), mimateo@upv.es (M.Á. Mateo), barmcar@upv.es (B. Armengot).

https://doi.org/10.1016/j.applthermaleng.2023.120910
Received 30 November 2022; Received in revised form 9 May 2023; Accepted 8 June 2023
Available online 17 June 2023

are two additional methods. Other more sophisticated models considering advection (moving finite line-source models (MFLS)), [20,21], or semi-numerical electric analogies, [22,23], are present in the market but the absence of data usually limits their practical applicability.

Most of this models require that the thermal power injected into the BHE remains constant throughout the experiment. This constraint is achieved by controlling the flow through the BHE and increasing, usually with an electrical heater, the inlet BHE temperature, calculated as the outlet temperature plus a required fixed value. In [1,24] it is described in detail the process of performing a TRT and how the outcome of the ILS and FLS models is affected by the fulfillment of their assumptions (constant power rate, positioning of the temperature sensors, sensors accuracy, etc.).

Even if all the constraints of the models are fulfilled strictly while performing a TRT, there are, however, serious difficulties when using some of these models. For instance, in ILS, the estimated values for the BHE parameters and ground properties (represented by its borehole thermal resistance, R_b, and ground thermal conductivity, λ, respectively) tend to spread and depend on the data window chosen, adding arbitrariness into our estimates if thermal oscillations caused by diurnal variations in temperature are not sufficiently isolated, [25,26]. Additionally, there is a high correlation between R_b and λ [27], leading to ambiguous parameter identification. The fact that the models only functions during intervals that are lower-bound by a specific timescale, often in the range of 6 to 20 h, presents another challenge because it requires discarding early-time, non-useful data. The borehole resistance, as defined in ILS and FLS, is essentially a synthetic composite parameter and not a material attribute; rather, it is only indirectly related to physical and measurably existing quantities.

Nevertheless and despite all these shortcomings, when combined with strict guidelines and proper analysis, TRT is an essential instrument in SGE day-to-day applications to gather information about the overall long term heat transfer of a given BHE. Its use should be strongly encouraged and promoted [28].

Apart from market considerations, the restriction on the shorter time scale of the models currently used for TRT analysis makes them useless for comprehending short-term, close-proximity properties of the BHE separately and, therefore, it is challenging to apply them to confirm the benefits that ongoing research programs claim to achieve by using new advanced materials and geometries intended to promote heat transfer to the ground.

FLS and MFLS models, as introduced before, are conditioned by the same short-scale limitation while other concepts, such as the use of more sophisticated semi-numerical approaches, typically tend to require the adjustment of many internal model parameters (in the form of resistances) and produce good fitting with experiment data but not a very clear insight into the physical processes inside the BHE.

Recently, a different strategy was investigated by some authors in the context of TRT analysis, [29–31], derived from a classical solution of the off-centered infinite line-source composite cylindrical two regions heat conduction transfer problem found in the classic textbook of Carslaw and Jaeger [32].

The primary distinction is that each zones (within and outside the drilling radius) has its heat conduction problem solved, and the resulting picture of temperature evolution over short and long periods of time is nearly complete. It is dependent on four variables (the conductivity and diffusivity of the soil and grout) instead of the usual two parameters in ILS, providing insights into the grout's characteristics.

Composite two-region line-source (C2RLS) frameworks represent thus a promising solution to the standard TRT practice's short timescale problem and to the challenge of obtaining meaningful grout-related parameters like conductivity and diffusivity. As a drawback, their formulation is more intricate compared to the ILS, FLS, and MFLS techniques, which might represent a significant barrier to its use. Li and Lai's original article [30] noted that some numerical calculations and simplifications are required. However, they demonstrated, [33,34], the method's applicability to determine some of the main ground and backfill properties in a sandbox setup with tightly controlled, high-quality measurements. Despite this, C2RLS has not yet seen widespread use in practical applications.

Our study was prompted by the need to assess potential changes resulting from the use of various plastic materials, geometrical arrangements, and grout recipes inside different BHEs. These new materials and configurations are outcomes of the European H2020 project GEOCOND [2], and were installed in our test field at the Universidad Politécnica de Valencia (UPV) [24,27,35], as well as in other different locations in Europe.

In order to address the limitations of standard TRT approaches for accurately assessing the potential benefits of new materials in BHEs, plausible parameter sets were identified to represent the distinct temperature responses of each BHE. Plausibility requires parameter values to lie within the admissible physical limits, to be reasonable (i.e. in accordance with previously known, reliable information), and to allow a proper prediction of the dynamic temperature response of the BHE.

To achieve the stated objective, the C2RLS formulation was adapted to extract relevant ground and backfill information from a combination of steady and unsteady thermal injection pulses. As the so obtained parameters are directly correlated with actual physical quantities, our method allows to formulate plausibility criteria to identify solutions that not only allow to predict temperature responses suitably, but as well represent meaningful solutions.

Altogether, these tools can obtain excellent predictive models based on plausible and consistent grout and soil parameters that showcase the benefits of the materials and measures developed within GEOCOND project.

The conclusions of this research not only provide an insightful perspective about the advantages of the new grouting and plastic pipes (improving substantially the operational performance of a borehole by optimizing the materials of its individual components (pipes, grout,..) with a direct impact on cost savings in installation and operation, enabling a significant increase in the economic benefits associated with shallow geothermal technology [4]), but also extend the amount of information that can be obtained from TRT analysis in realistic test environments.

The paper is structured as follows. Section 2 describes the models used to obtain the final g-functions allowing the analysis of experiments. Besides the g-functions as obtained by other authors, we explain the need to look more accurately at small Fourier numbers. Following, Section 3 describes the different BHEs and related experiments. To tackle the parameter identification problem, in Section 4 a new approach, combining steady and unsteady C2RLS analysis will be introduced for the analysis of data obtained by means of TRT and describes the application of C2RLS based functions to the new boreholes developed within EU project GEOCOND, using also previously tested BHEs as reference. Section 5 summarizes the final conclusions of our paper. A more detailed account of some important mathematical details is found in Appendix A, containing a description of the C2RLS method.

The experimental data, computed g-functions and required instructions to perform the calculations will be made available to the broad community of researchers through an *Opendata* project (see Appendix B).

2. Homogeneous versus composite 2-region ground thermal response analytic models

2.1. Analytic approach for TRT analysis using an homogeneous region and a line source

A typical TRT heat injection setup consists of a closed circuit with a pump, a water tank and a heating appliance connected to the BHE. A heat carrying fluid (usually water) enters the borehole heat exchanger at a given temperature T_{in}. After exchanging heat with the soil, it leaves

the BHE at a temperature $T_{out} < T_{in}$. A basic requirements is that the heat injection $\dot{Q} = \dot{v}\, c_f\, \rho_f (T_{in} - T_{out})$ shall be kept constant, being $\dot{v}$ [m^3/s] the heat carrier fluid (volumetric) flow, ρ_f [kg/m^3] its density and c_f [$J/kg\,K$] its mass specific heat capacity.

As a response to heat injection there is a time varying increase of the underground temperature. All TRT analysis schemes are based on the establishment of a relationship between the directly observed increase of the arithmetic mean temperature in the carrier fluid inside the BHE ($\bar{T}_{exp} = \frac{1}{2}(T_{in} + T_{out})$) with the forecast increase in underground temperature.

One particular way is the ILS approach, [17,36,37], which considers a heat flow rate per unit length of the borehole $\dot{q}_L = \frac{\dot{Q}}{H}$, where H is the borehole length, applied to a linear source of infinite length extending towards the negative half-space ($z \leq 0$), and a medium that is semi-infinite and porous, initially at thermal equilibrium at the undisturbed temperature T_0. Soil thermal properties are independent of the temperature and the boundary of the ground surface is considered at the same fixed temperature. The natural geothermal gradient is not considered.

The directly observed increase of the arithmetic mean in the carrier fluid temperature, T_{exp}, is equal to the temperature calculated at the lateral surface of the borehole (i.e. $r = r_b$) plus the corresponding fixed increase due to the borehole resistance and given by:

$$\begin{aligned} T_{exp}(t) &= \Delta T_{ILS}(r_b, t) + \dot{q}_L R_b + T_0 \\ &= \frac{\dot{q}_L}{4\pi\lambda} E_i\left(-\frac{r_b^2}{4\alpha t}\right) + \dot{q}_L R_b + T_0 \\ &\approx \frac{\dot{q}_L}{4\pi\lambda}\left(\ln\frac{4\alpha t}{r_b^2} - \gamma\right) + \dot{q}_L R_b + T_0, \end{aligned} \tag{1}$$

where the function $E_i(u)$ denotes the exponential integral, [32], γ is the Euler–Mascheroni constant. Ground conductivity and diffusivity are denoted λ and α, respectively. It is important to highlight that Eq. (1) is valid for times larger than 5 times $t_b = r_b^2/\alpha$, usually in the order of some hours to 1 day, [18,36], whereas typical thermal test duration's range from 40 to over 200 h. [12,38].

In addition, there is some literature, [39], to close the gap by providing formulations to relate R_b to the dimensions (shank spacing), material properties or BHE specifications in general.

As explained in the introduction, there have been several extensions of this approach (FLS, CLS, MFLS) to take into account more realist considerations and effects such as groundwater advection. Normally these corrections are relevant on a longer time-scale and, in the scope of the present work, they will not be further covered here.

2.2. Composite-medium 2 region line source framework, C2RLS

In a composite-medium model heat conduction due to an instantaneous line-source of infinite length is solved by an old approach due to Jaeger [32], considering an infinite composite solid region expressed in cylindrical coordinates divided into two cylindrical subdomain regions, $r \leq r_b$ and $r > r_b$, with media of different physical properties (see Fig. 1). Alike ILS, an infinite line-source of strength $\dot{q}_L$ constantly releases heat into the composite solid from zero time. The line-source is parallel to the height direction, z-axis, located through a point (r', θ'), not necessarily in the center of the internal cylinder region. The observation point in which the temperature response is measured or computed is given by $(r, \theta$ in cylinder coordinates.

Instead of considering the region beyond the borehole radius, the C2RLS approach allows to model the temperature at the surface of the BHE probe and only one fixed resistance must be considered, namely the heat resistance through the pipe-wall of both single U-tube legs, R_p.

The temperature of the fluid is then given by:

$$T_{exp}(t) = \Delta T_{C2RLS}(r_p, t) + \dot{q}_L \frac{R_p}{2} + T_0, \tag{2}$$

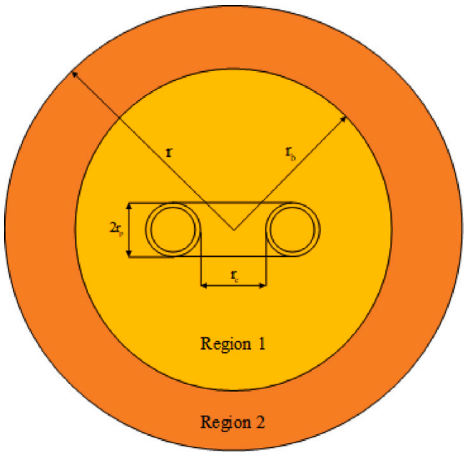

Fig. 1. 2D schematic of Composite-medium 2 Region Line Source framework, C2RLS.

where the factor 2 accounts for the fact that there are two pipes through which heat flows in parallel with fluid-pipe heat resistance equal to R_p. The varying temperature difference is now to be calculated at the pipe radius r_p instead of r_b.

The following paragraphs summarize the main features of the non-dimensional temperature response for the C2RLS single-U BHE case. A more comprehensive model description can be found in Appendix A. Relevant literature for the TRT analysis of the model includes the work of Carslaw [32] and its more recent adaptation to TRT analysis due to Li and Lai [34,40].

For the following, it is found to be convenient to write the temperature response in non-dimensional terms as $\Theta_i = \frac{2\pi\lambda_i T_i}{\dot{q}_L}$, where the sub index i is equal to 1 for the temperature response in the inner region, while sub-index 2 corresponds to the response in the ground region, outside the core.

The temperature response is function of three non-dimensional quantities. The first relates to time and is the Fourier number related to the borehole radius. In region 1 it is given by $\mathrm{Fo} = \alpha_1 \frac{t}{r_b^2}$, where α_1 is the backfill diffusivity.

Two additional dimensionless quantities play an important role, parameter $k = \frac{\lambda_2}{\lambda_1}$, which corresponds to the ratio of grout to ground conductivity, and the ratio of volumetric heat capacities of ground and grout defined by:

$$\phi = \frac{c_{v2}}{c_{v1}}.$$

In contrast to the approach taken in Li's work [40], the decision has been made to utilize the variable ϕ instead of the ground-to-grout diffusivity ratio parameter a (as described in Appendix A). Although these two parameters are closely interconnected, since a can be expressed as $a = \sqrt{\phi/k}$.

By means of the Laplace transform method, the heat equation and specific boundary conditions can be expressed explicitly and an analytic solution for the heat step can be written. In [40], equations (4a) and (4b) (corresponding to Eqs. (A.1) and (A.2) in Appendix A), a solution is given for both regions, inside and outside the BHE core region. The corresponding solutions for regions 1 and 2 are given by the non-dimensional temperature response functions $\Theta_1(\mathrm{Fo}, R, \theta)$ and $\Theta_2(\mathrm{Fo}, R, \theta)$ and describe the varying time response as a function of time (through the corresponding Fourier number), the non-dimensional observation point distance $R = r/r_b$ and its angular position in cylinder coordinates given by θ. In order to calculate temperatures at the BHE wall only the solution valid for region 1 is required.

The overall response of a single-U BHE is represented by the superposition of two linear sources located at cylinder coordinates $(r_c, 0)$ and (r_c, π). The observation point coordinates can be related to the non

dimensional shank spacing ($\eta = r_c/r_b$) and the non dimensional pipe radius ($\rho_p = r_p/r_b$). With the above notation, after some simplifications described further in Appendix A, the overall non-dimensional temperature response of a single-U heat exchanger can be expressed as follows:

$$\Theta_{SU}(Fo,\eta,\rho_p,k,\phi) = \sum_{n=0}^{+\infty} \mathrm{K}_{2n}(Fo,\eta,\rho_p,k,\phi), \tag{3}$$

where the list of functions K_{2n} classified according to n (being n a natural number $n = 0, 1, 2\cdots$) is given by:

$$\mathrm{K}_{2n}(Fo,\eta,\rho_p,k,\phi) = \int_0^{+\infty} (1-e^{-\upsilon^2 Fo})\times \frac{2kJ_{2n}(\upsilon\rho_p)(J_{2n}(\upsilon(\eta-\rho_p))+J_{2n}(\upsilon(\eta+\rho_p)))}{\pi^2\upsilon\left(\mathbb{A}_{2n}^2+\mathbb{B}_{2n}^2\right)}d\upsilon, \tag{4}$$

and where,

$$\mathbb{A}_{2n} = (ak\upsilon J_{2n}(\upsilon)J_{2n-1}(a\upsilon) - J_{2n}(a\upsilon)((k-1)2nJ_{2n}(\upsilon)+\upsilon J_{2n-1}(\upsilon)))$$
$$\mathbb{B}_{2n} = (J_{2n}(\upsilon)((k-1)2nY_{2n}(a\upsilon) - ak\upsilon Y_{2n-1}(a\upsilon)) + \upsilon J_{2n-1}(\upsilon)Y_{2n}(a\upsilon)),$$

being J_n and Y_n the nth Bessel functions of first and second kind.

Eq. (3) can be approximated numerically, but is cumbersome to obtain in comparison with expressions such as Eq. (1).

To ease and speed up computation, we constructed, by interpolation, a multidimensional *surrogate* temperature response function - $\tilde{\Theta}_{SU}$ - to approximate the Θ_{SU}-function given by Eq. (3). For this, the original function was calculated in a certain number of sampling points within a region of interest in the $(\mathrm{Fo}, k, \phi, \eta, \rho_p)$ parameter space. This domain of relevant parameter values is of a limited extension and is analyzed at the end of Appendix A to determine its boundaries.

Logarithmic time-sampling was selected for the evolution of the temperature vs. the Fourier number in order to properly capture the fast evolution at small time-scales. The rest of non-dimensional parameters in the model, namely (k, ϕ, η, ρ_p), were sampled linearly in their respective intervals. In the case of k and ϕ, a previous analysis was done in order to select feasible values for these coordinates.

To obtain the surrogate C2RLS temperature response function for a single-U BHE, $\tilde{\Theta}_{SU}$, an approximate value of the exact function was calculated for a total of about 70.000 points within the relevant domain, by using equation (A.9) (see Fig. 2). Then, by means of spline-interpolation, a smooth, differentiable, interpolating function was calculated that approximates the exact $\tilde{\Theta}_{SU}$.

One decisive advantage is that the surrogate function shall be calculated only once. It then can be used to model any possible single-U BHE configuration by adequate choice of the η and ρ_p parameters. Hence, once the $\tilde{\Theta}_{SU}$ is obtained, the C2RLS model can be used conveniently and is reasonably easy and fast to compute. The final model reads (for a fixed single-U geometry, i.e. given values of η and ρ_p):

$$T_{\mathrm{C2RLS}}(t;\lambda_1,k,\phi) = \frac{\dot{q}_L}{2\pi\,\lambda_1}\tilde{\Theta}_{SU}(\mathrm{Fo}(t),k,\phi) + \dot{q}_L\frac{R_p}{2} + T_0, \tag{5}$$

which can be adjusted to minimize some error objective function to identify a set of optimal $(\lambda_1, k, \phi, R_p, T_0)$ values.

In principle, the pipe heat resistance, R_p, can be used as a free parameter to be fitted, or estimated independently, as it involves well-characterized sequential heat transfer processes. This represents a substantial advantage in comparison to conventional line-source methods, where the free parameter R_b cannot be unequivocally linked to mensurable quantities.

Indeed, as a reference value for R_p, a theoretical pipe heat resistance, R_p^*, can be calculated as a function of the pipe inner and outer diameters, $r_{i/o}$, the Nusselt number characterizing forced convective heat transfer from the fluid to the pipe wall (Nu) and conductivity of the pipe material and heat exchange fluid inside the BHE ($\lambda_{p/f}$) by the following well-known expression:

$$R_p^* = \frac{1}{2\pi\,\lambda_p}\log\frac{r_o}{r_i} + \frac{1}{\pi\,\lambda_f\,\mathrm{Nu}} \tag{6}$$

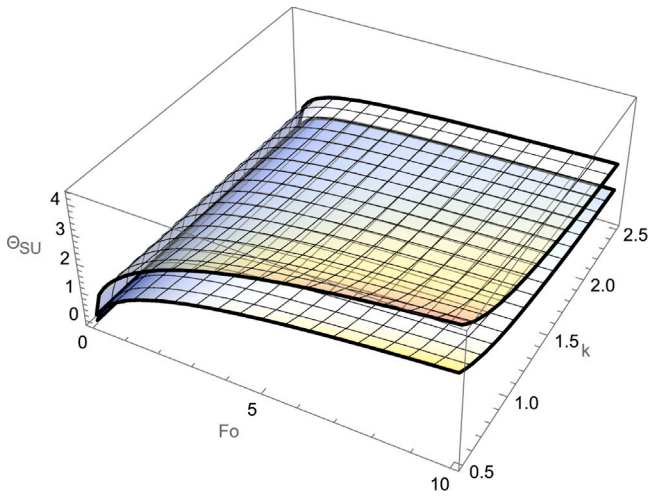

Fig. 2. 3D-representation of the surrogate $\tilde{\Theta}_{SU}$ function for varying values of the Fourier and k parameters and fixed values of the rest of parameters (ϕ, η and ρ_p). Specifically, the upper, transparent, sheet corresponds to $\phi = 0.4$, $\eta = 0.4$ and $\rho_p = 0.25$, whilst the lower sheet was calculated with: $\phi = 1.2$, $\eta = 0.7$ and $\rho_p = 0.25$.

The correlations recommended by the 2010 version of the comprehensive VDI guidelines, Verein Deutscher Ingenieure (English: Association of German Engineers) [41] have been applied to calculate the Nusselt number as a function of the Reynolds and Prandtl numbers. These correlations are applicable for laminar, intermediate and turbulent flow regimes. The limit of a smooth pipe has been assumed in all cases with respect to the rugosity of the inner wall of the pipe.

Through proper estimation of the Fourier number $\mathrm{Fo} = \frac{\alpha_1 t}{r_b^2}$ it would be potentially feasible to estimate α_1, i.e. grout diffusivity, through a fitting of data to the theoretical model given by Eq. (5). Then, the simultaneous estimation of ϕ and k allows to obtain estimates for all basic ground properties of backfill and surrounding ground (conductivity, heat capacity and diffusivity). However, this estimation is plagued with difficulties, as already highlighted in [31], due to the parameter identification issues to be discussed in the next paragraphs.

Before entering into the question of parameter identification, how the newly developed g-functions can be used to adjust the thermal response in real-life, steady injection tests with improved accuracy compared with conventional methods will be shown.

To that aim, we re-analyze – by means of the new functions – steady injection TRT data from experiments that were reported and thoroughly analyzed in previous work [27] and are briefly summarized in table 2 in Section 3.

2.3. Application of the C2RLS algorithm to a long-term steady injection experiment

During April 2017 a 815.18 h duration (32-day) constant heat pulse injection was performed in a test borehole inside the UPV campus. For the present research, the data set obtained has been used to test the applicability of the composite 2 region g-functions obtained in the previous sections, and to compare the results with those obtained by application of homogeneous heat transfer region models based on ILS, FLS and MFLS. A sample of the obtained results is shown in Fig. 3, (it corresponds to test identifier O1 T2 in Table 1, in Section 3) where, in contrast to the original figure in [27], here a logarithmic timescale is used to better highlight the behavior of the different models at shorter time scales.

For model adjustment the first 72 h of data were selected as upper time limit for parameter estimation (simultaneously, as explained in [27], the first 24 h of data were disregarded). From this data window,

Table 1
Tested BHE size, dimensions and materials.

BHE #	Pipe material	Pipe conductivity [W/(mK)]	Grouting	Grout conductivity [W/(mK)]	Diameter [mm]	Depth [m]	Casing
O 1	PE100	0.37*	CEMEX 32.5 raff	–	160	39.5	No
N 1	PEX	0.41*	Std Commercial grout	2*	126	14.6	No
N 3	Enh. plastic	1.02**	Enhanced grout	2.17**	140	12.0	Yes
N 5	PE100	0.37*	Enhanced grout	2.23**	140	11.4	Yes

* Nominal value given by manufacturer.
** Measured from samples taken in-situ during backfilling operations.

Table 2
Main thermal test parameters corresponding to the TRT included in this research.

BHE #	Test identifier	Test date		Nº of inj. steps	Max. thermal injection		Flow rate	Duration
		Month	Year		Ratio [W/m]	Total [W]	[m^3/h]	[h]
O 1	O1 T1	March	2016	2	50.56	1997.14	0.479	267.1
	O1 T2	April	2017	2	62.06	2451.4	0.293	815.18
N 1	N1 T1	Jan	2018	3	79.43	1159.5	0.250	121.1
	N1 T2	May	2022	5	79.43	1159.5	0.250	121.1
N 3	N3 T1	July	2022	5	79.93	959.2	0.300	192.78
N 5	N5 T1	Nov	2021	5	89.83	1024.0	0.258	332.33
	N5 T2	May	2022	5	79.98	911.82	0.292	164.1
	N5 T3**	Feb	2022	18	100	1140	0.296	83.31

* Water properties at 40 °C: density 992.3 kg/m^3 viscosity 0.000653 kg/(ms).
** Validation test; not intended for parameter estimation.

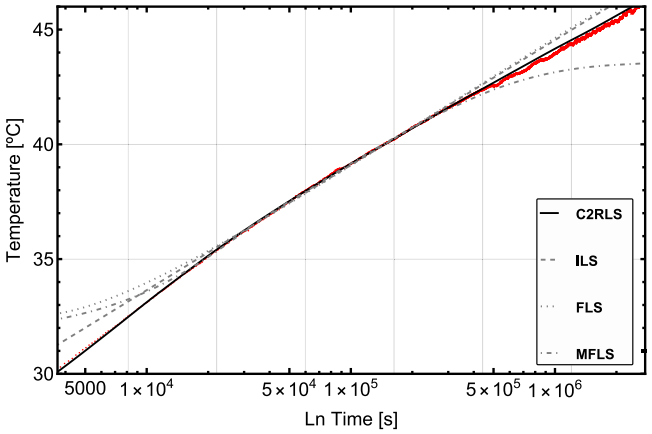

Fig. 3. Results of model fitting of the 32 day O1 T2 TRT experimental data. Four different theoretical models have been used. The three homogeneous line-source model already included in the analysis of [27], ILS, FLS, MFLS, are complemented with the results of the C2RSL model fitting. Experimental data are shown as red dots. In all cases the parameters for the models are obtained after 72 h and the projection of the model to the full measurement period is shown.

parameters were estimated and the resulting extrapolation is depicted, showing a reasonable match in the case of ILS and FLS methods (and an inadequate estimation in the case of MFLS). However, as expected, at short time scales (below about 3×10^4 s) the only model that closely follows the experimental trend is the one based on the composite 2 region line source g-functions (in this case C2RLS functions were used).

With the above comparison, we have shown that C2RLS outperforms traditional linear source approaches in adjusting or predicting temperature trends in TRTs performed under real field conditions. However, it is far from evident that C2RLS can provide a practical framework to obtain soil and grout parameters that are useful for BHE modeling and TRT practice. The main reason, as previously pointed out in [31], is that unambiguous parameter identification is challenging when modeling TRTs in general.

To overcome this difficulty a good model is not sufficient and it is necessary to address the common difficulties in engineering that arise when estimating parameters in models using experimental data.

3. Thermal response tests description

3.1. Geological setting

The test field area is geologically characterized by an alluvial environment dominated by the sedimentation of siliciclastic materials with varying granulometries, resulting from the activities of rivers and ravines. These materials form an aquifer that has been described as the Aquifer System of Plana de Valencia in the hydrogeological map of Spain [42]. The materials are considered permeable to semipermeable, allowing a continuous groundwater flow towards the sea, as suggested by the hydrogeological map and local records of piezometric levels in several wells and control points.

We have established the thermal characteristics of the ground based on literature information [43,44] regarding the dominant sediment types in the study area, such as gravel lenses with silty sands and clays (see [45]).

3.2. Description of the test sites and boreholes

Measurements were performed in two different nearby sites located both at the Universitat Politècncia de València (UPV). The initial test site (termed herein, “O”) was set up to perform long term TRT experiments with accurate injection control and is equipped with an electric powered 3 kW thermal injection system. In section 2.1 of [24] and in [27] the system was extensively described, consisting of two single-U’s pipes inserted into a single borehole. Only the deeper one, 39.5 m pipe, was used for the purposes reported here.

The second test site (“N”) is dedicated to the study of a variety of different BHE configurations as part of various past and ongoing projects. Up to date, 13 different BHEs are installed, all of them connected to a remotely accessible, PID–based heat injection system that allows a tight control of heat injection. The “O” and “N” fields and measurement systems have been described in a previous publication

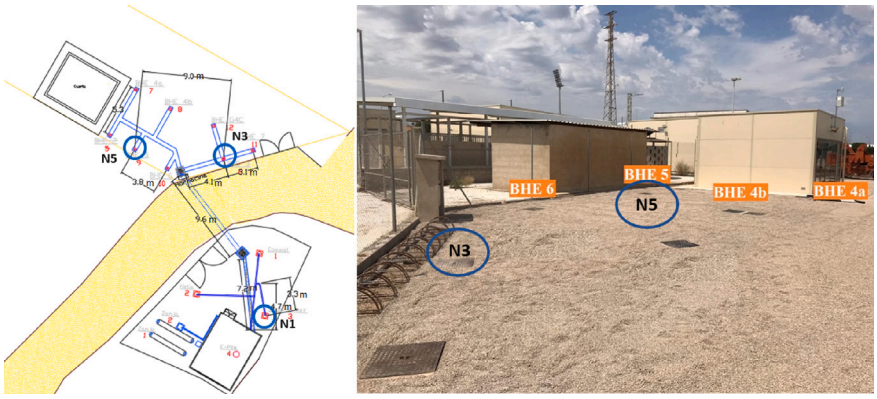

Fig. 4. N borehole field (test site). The left side represents a map of the *N* test site, where the arrow corresponds to the approximate position from which the right image was taken. The location of N 1,3 and 5 is depicted. The single–U BHE shown at the bottom of the image is a single-U reference BHE (N 1) installed with conventional grouting and piping.

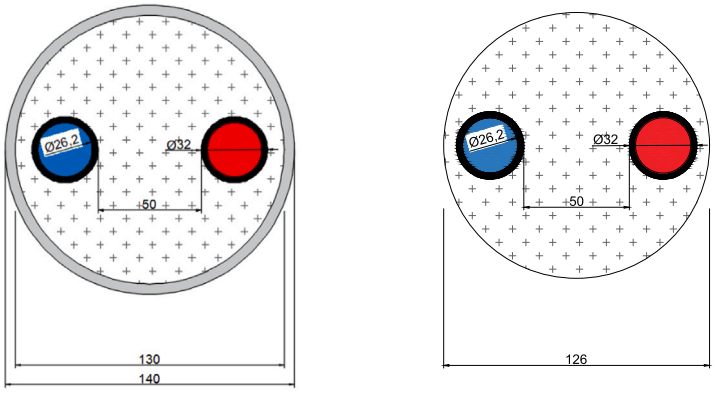

Fig. 5. Section of the borehole with **(a)** 140 mm diameter **(b)** 126 mm diameter.

with some detail, see [45]. Only essential additional information will be included hereafter.

In Fig. 4, the left image displays the location of several boreholes that were studied in this research. The right figure shows a map of the "N" boreholes. The single-U BHE shown at the bottom of the left image is the single-U reference BHE (N 1), installed using conventional state-of-the-art grouting and piping, serving as a useful reference for comparing the differences due to the new grout and pipe materials in boreholes N 3 and N 5. The distances between the heater tank and the different BHEs are 8 m, 22.6 m, and 20.09 m for N 1;N 5 and N 3 respectively. The distances, however, do not pose a problem since each BHE is equipped in its head with temperature sensors on the inlet and outlet of the heat exchanger.

Table 1 and Figs. 5(a) and 5(b) specify the essential geometric configurations and basic material characteristics of each of the BHE options included, such as the kind of pipe material, the grouting mix injected in the borehole, as well as its nominal diameter and depth. Besides, other important details for calculation are to be mentioned. In the case of N 1, the borehole shank spacing is about 82 mm, whilst N 3 and N 5, shank spacing is of about 40 mm. In both cases plastic pipe thickness was 2.9 mm (see Fig. 5(b)).

3.3. Test configurations

The tests included in the present study are presented in Table 2. Due to the different types of heat injection, the control in the case of the O 1 tests is substantially different compared to the N 1, 3 and 5 experiments. In the case of O 1 the heating element is an electric resistance that provides a stable and constant thermal power injection. The system is extremely compact and all parts are well insulated, therefore external disturbances can be minimized.

Ambient influences and other perturbations are more difficult to control in the case of the "N" site boreholes, as the system is fed by a warm tank located at a much larger distance from the BHEs (see Fig. 4). The preset thermal power injection is regulated by a PID controller fed by a signal depending on the inlet/outlet temperatures measured just at the corresponding borehole. A control algorithm allows to obtain stable injections, as an essential condition for accurate analysis. It is also important to mention that flow rates are set in order to ensure turbulent flow and, simultaneously, a large enough temperature difference across the BHEs to avoid significant error due to uncertainty in the temperature measurement.

To obtain an unsteady injection temperature record according to the description outlined in Section 4.3, there are several basic injection scheduling schemes utilized to implement our approach. A first scheme was used along the O test site, which consists of using the temperature records of the several hours long initial circulation that was performed before the start of the steady TRT injection pulse.

In tests with N 1, 3 and 5 one or several injection pulses of different duration were used. Typically five injection periods were recorded: pumping without heat injection, a first injection at the preset nominal power lasting 72 h, pumping without injection for further 24 h, a further injection of 24 h at 70% of the chosen nominal power and a final period of pumping without injection of 24 h.

To represent the different programs in Table 2, the number of heat injection periods is represented ranging from a minimum of 2 in the

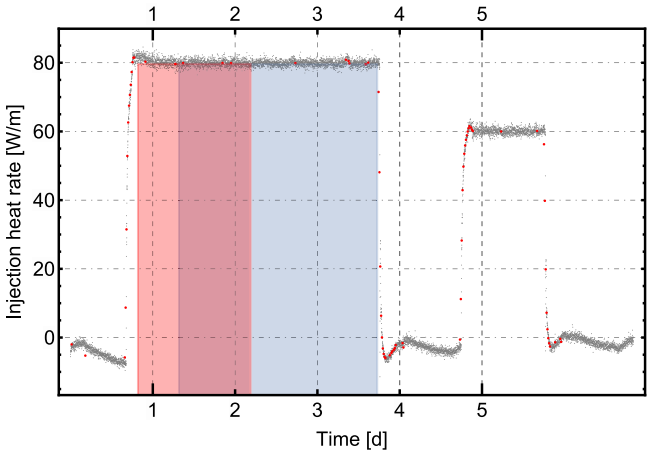

Fig. 6. Heat injection partitioning as input for the estimation procedure with data of test N5T2. The cloud of small gray dots represents the instantaneous heat injection recorded from the sensors. The red dots represent the points selected by the partitioning algorithm as input to the heat injection function for the parameter estimation. The partially overlapping segments shown as a red and blue region show the data intervals used to fit the C2RLS and ILS algorithms, respectively. The horizontal time scale is in units of days.

"O" test site tests, to a maximum of 18 used for a final validation test with N5. In Fig. 6, as already discussed, two examples of such heat injection rate programs are shown, and the periods for C2RLS, ILS and unsteady data analysis are depicted according to the method outlined in Section 4.3.

4. Results and discussion

4.1. The identifiability challenge

Identifiability of models is a topic well studied in some areas of engineering and statistics, [46,47], where frequently the experimental analysis shows *structural* issues (because the way the model is set does not allow to identify parameters separately) or *practical* (because model parameters can be in principle inferred, but the result is extremely sensitive to noise due to the specific correlations that appear between variables). Partly, this behavior of models is related to the concept of parameter sensitivity, i.e. how much temperature is changed with respect to the change of a given parameter value.

If a model that estimates the dependence of temperature on time, t, and depends on a list of n parameters $(p_i; i = 1, \dots, N)$ is in the form:

$$T = T(t; p_1, p_2, \dots, p_N)$$

The parameter sensitivity with respect to a change of a certain parameter p_i is in general defined as, [46]:

$$X_{p_i} = p_i \frac{\partial T}{\partial p_i} \qquad i = 1, \dots, N.$$

Owing to this definition, all sensitivities, X_{p_i}, derived from any of the parameters p_i are expressed as temperatures, which allows direct comparison. For parameter estimation, it is desirable that sensitivities are large, for if a parameter shows a small sensitivity, its variation must be large to produce a noticeable effect on temperature estimation, being strongly affected by small changes in the experimental conditions, by the presence of uncertainties and by experimental errors.

When attempting to estimate a feasible set of values for the p_i parameters from a collection of M observations $T_{exp;i}$ measured at times $t_i, i = 1, \dots, M$ - as analyzed in the context of C2RLS by Li and Lai, [31], following the general discussion in [46] - a further problem appears when there is a linear relationship amongst the different variation vectors given by:

$$\frac{\partial \vec{T}}{\partial p_i} = \left(\left.\frac{\partial T}{\partial p_i}\right|_{t=t_1}, \left.\frac{\partial T}{\partial p_i}\right|_{t=t_2}, \dots, \left.\frac{\partial T}{\partial p_i}\right|_{t=t_M} \right). \qquad i = 1, \dots, N$$

If, see [47], the situation is found that, for a given subgroup of two or more parameters, p_i , $i = n, \dots, m$ (where $n \geq 1$ and $m \leq N$) its variation vectors are linearly dependent, meaning that the following expression holds for a certain non-trivial election of coefficients a_j:

$$\sum_{j=n}^{m} a_j \frac{\partial \vec{T}}{\partial p_j} = 0, \tag{7}$$

then the p_i parameters cannot all be uniquely estimated. It will be shown in the following that this is the case for both linear-source and C2RLS models.

4.1.1. Identifiability issues in homogeneous line source analysis

When considering ILS analysis, it is well known that a fixed reference ground diffusivity and an independent true evaluation of the undisturbed ground temperature must be established. This is to some extent a "chicken-and-egg" situation, for α is normally as unknown as the target ground conductivity parameter λ.

Let us consider that, to perform an estimation by means of ILS, a reference $\bar{\alpha}$ diffusivity and an undisturbed ground temperature, $\bar{T}_0$ must be chosen.

If α is the true ground diffusivity and T_0 the true undisturbed ground temperature, from expression (1) it can be verified that the relationship between the (incorrect) borehole resistance $\bar{R}_b$ related to the chosen values $(\bar{\alpha}, \bar{T}_0)$ with the respect to the true borehole resistance is given by:

$$\bar{R}_b = R_b + \frac{T_0 - \bar{T}_0}{q_L} + \frac{1}{4\pi\,\lambda} \log(\alpha/\bar{\alpha}). \tag{8}$$

Furthermore, as (α, T_0, R_b) are constant, condition (7) is satisfied for this group of three parameters.

Hence, from expression (8) as well as from the general identifiability criteria given by expression (7) it follows that it is not possible to uniquely estimate these three parameters.

Borehole resistance is ambiguous unless an *independent* valid estimate of the undisturbed ground temperature T_0 and the ground diffusivity α is provided.

A further source of ambiguity in homogeneous linear source analysis is the need to specify a lower time threshold below which the calculation is not applicable. This time window selection effect has been extensively discussed by several authors, see f.i.[26], as highlighted in the introduction and different countermeasures have been proposed.

4.1.2. Parameter identifiability in the C2RLS framework

Since C2RLS analysis is based on a stable heat transfer between the fluid inside the pipes and the part of the grout beneath the pipe, which is established in around 10 to 20 min, [40], the type the selection of a lower time-bound affects only initial data and does not influence parameter estimation significantly.

Furthermore, see Eq. (5), the important role of the estimation of an undisturbed ground temperature is still an issue, as well as the pipe resistance R_p. As the model asymptotically behaves similarly to the ILS, the diffusivity can be expected to be subject to similar confusion.

However, in this regard the situation is quite different in comparison to homogeneous linear source approaches. A clear way of estimating the value of the R_p resistance is through the use of well-known independent physical laws, such as Eq. (6). On the other hand the structural role of the diffusivity is quite more complex in C2RLS modeling and its sensitivity varies along time. In general, the fact that in C2RLS all quantities obtained relate to actual physical and mensurable material properties is a definitive advantage particular to this scheme.

Table 3
Parameter estimation based on tests with the best Standard Deviation.

Test identifier	Conductivity		T_0	Diffusivity ($\times 10^6$)		R_b	R_p^*	Std Dev
	Ground [W/mK]	Grout [W/mK]	[°C]	Ground [m²/s]	Grout [m²/s]	[mK/W]	[mK/W]	[K]
O1 T1	2.37	0.65	20.64	0.93	0.37	0.195	0.0815	0.046
O1 T2	2.37	0.65	20.56	0.91	0.246	0.192	0.108	0.029
N1 T1	2.20	0.94	19.82	1.02	0.219	0.121	0.100	0.421
N1 T2	2.42	0.84	20.40	1.17	0.243	0.126	0.100	0.097
N3 T1	4.06	1.17	21	1.71	0.445	0.115	0.0566	0.272
N5 T1	3.04	1.33	21.24	1.27	0.18	0.108	0.0991	0.151
N5 T2	3.27	1.37	20.96	1.61	0.22	0.107	0.0991	0.058

* Theoretical estimate of the pipe resistance based on eq. (6).

A further issue, analyzed in deep by Li and Lai, [34], relates to the fact that the non-identifiability condition given by Eq. (7) is satisfied in the sensitivity analysis of a group of C2RLS parameters throughout a substantial time window. Their sensitivity analysis of the model parameters (see Figure 6 in Ref. [34]) shows how four of them ($\alpha_1, \alpha_2, \lambda_1$ and η) become constant and thus linearly related after 10 h of injection. From this model feature the authors conclude that if only later-time data of a TRT were used in a parameter estimation, it would be impossible to determine them simultaneously. According to these authors: "nonlinear feature of X within short times ($t < 10$ hr) can greatly reduce the linear dependence of the parameters and thus greatly improve the identifiability".

A strategy combining the use of steady and unsteady heat injection analysis is proposed to tackle the identifiability problem and obtain an improved identification of parameters.

4.2. Unsteady C2RLS modeling

By using a time dependent rate of injection, the sensitivity functions related to R_p and T_0 are not longer strictly proportional, as $\dot{q}_L$ is a function of time. Also the linear dependence between the model parameters sensitivities, as highlighted before, is limited.

To adapt the model as described in Eq. (5) for use with non-stationary injection, following Duhamel's theorem, [32], a solution is constructed by a step-wise superposition of constant-injection solutions. Assuming that the load of a given BHE is a function of time $q(t)$, the unsteady temperature evolution is in general given by:

$$T_{USt}(t) = T_0 + \int_0^t q(\tau)\frac{\partial \tilde{g}_{SU}(t-\tau)}{\partial t} d\tau, \tag{9}$$

where:

$$\tilde{g}_{SU} = \frac{\tilde{\Theta}_{SU}}{2\pi\,\lambda_1} + \frac{R_p}{2},$$

represents the surrogate $\tilde{g}$-function, while $\tilde{\Theta}_{SU}$ is calculated from Eq. (3) by means of approximation, as explained in the previous sections.

By discretizing the heat injection signal into a number of constant heat pulses $\{q_1, q_2, \ldots\}$ starting at times $\{t_1 = 0, t_2, \ldots\}$ the particular expression is obtained:

$$T(t) = T_0 + q_1\,\theta(t)\,\tilde{g}_{SU}(t) + \sum_{i=2}^{N}(q_i - q_{i-1})\,\theta(t-t_i)\,\tilde{g}_{SU}(t-t_i), \tag{10}$$

being $\theta(t)$ the Heaviside function and q_i is the heat injection rate during the ith interval starting at $t = t_i$ (whereby $t_1 = 0$).

Since the number of intervals N affects speed of computation quite substantially, it is interesting to keep it as small as possible, but simultaneously, were changes in the injection rate are larger, more intervals should be placed to improve accuracy.

A possible approach is to choose more intervals where the $q(t)$ function changes more rapidly, that is, as a function of $q(t)$ variations. This is relevant when evaluating TRTs consisting on different constant heat steps, as is our case. In these tests, $q(t)$ might vary only slightly (due to noise or control) during long periods and change substantially during the transitions. As an application example, in Fig. 6 (corresponding to test N5 T2) a typical 5-step injection profile used for our test campaign is represented. The small red dots point to where the algorithm has placed a partition. The frequency and number of intervals can be adjusted by changing the sensitivity of the algorithm to variations of the measured heat injection rate $q(t)$. A good compromise between speed and accuracy was found by using around 200 q-intervals for a 6-day duration test with 5 injection steps.

4.3. Use of unsteady TRT data

The TRT must contain segments with different injection rates. The most simple option (followed in several of the cases discussed later) is to record temperatures data before injection starts at least during several hours. After start of injection, the usual TRT steady injection pulse is applied during a longer period, usually 72 h. A further option is to use sequences of injection pulses during which injected thermal power is kept constant. The first steady injection pulse must have a duration of at least 72 h to conform to standard TRT praxis, which enables evaluation by means of ILS (as ground must be initially undisturbed). It should be noted however, that the methods discussed here may not require such long periods of data acquisition, though this question will not be object of discussion in the framework of this analysis.

Our approach consists of two simple steps:

1. Using the steady injection part of the dataset, a constrained nonlinear fitting algorithm is used to obtain the set of parameters that minimize the Mean Least Square error (MLSE) between the steady C2RLS model and the data.
   To start the procedure, initial estimates for the undisturbed temperature and for the ground diffusivity T_0, α_1 are chosen. Feasible parameter estimations were produced by using the additional constraint that the volumetric heat capacity of the ground found by the fitting algorithm should fall within the range of known admissible values for the ground conditions.
   The first step produces as a result estimates for the ground conductivity (λ_2), the backfill conductivity parameter (λ_1) and the ϕ parameter (ratio between ground and grout heat capacities). The algorithm also finds an improved estimate for the α_1 grout diffusivity parameter which shall not depend on our initial guess. The pipe heat resistance parameter R_p is set at the theoretical value obtained from Eq. (6) and the undisturbed ground temperature T_0 is also considered fixed according to our initial estimation.
2. In the second part, the entire dataset is used to find an improved parameter estimation by means of constrained nonlinear model fitting of the C2RLS unsteady model, taking the parameters previously found as initial guesses.
   At difference with the first step, variation of T_0 and ϕ is permitted in order to achieve an optimal match between the model

and the data. The result is a full list of estimated ground and grout properties. As the new value for T_0 may affect the estimate obtained in the first step, at least one additional iteration is allowed, returning to step 1, but using the updated values of α_1 and T_0,. Usually one iteration is sufficient to find values that remain stable.

Finally, with the obtained ground properties, λ_2, T_0 and α_2 the steady part of the dataset is again used to obtain – by means of the ILS method and non-linear model fitting – an estimate for the borehole resistance, R_b, that is free from any unmotivated assumption.

Altogether, by means of the described method, a set of estimates is obtained that, in conjunction with the C2RLS unsteady model can be used to analytically predict the temperature response of a given BHE to any steady or non-steady heat injection or extraction sequence. These estimators are correlated (but should not be confused) with actual physical, mensurable soil and ground properties and can be compared with other estimation methods or literature values.

The application of this methodology to several thermal tests performed along several years in two test sites and four BHEs will be described in the next sections.

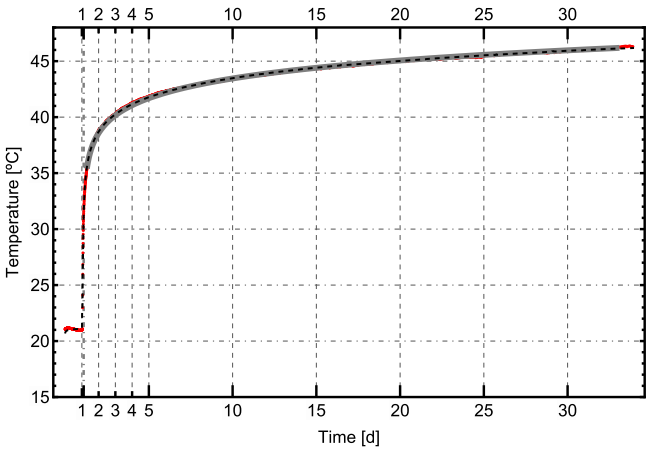

Fig. 7. Results of the data adjustment of the 32 day experiment O1 T2 in the linear time domain. The dashed line corresponds to the predicted trend given by the C2RLS unsteady model, while the gray curve shows the segment fitted with the ILS model. TRT data (average temperature in the borehole) are shown as red dots.

4.4. *O* 1 *results*

Plausible parameter set estimation. For both O1 tests, a set of solutions was generated starting from different prior values for T_0 and α_1. From these starting values it was left free to the algorithm to find parameters (including updated values for T_0 and α_1) that minimize the Mean Least Square difference between the model and the data. After a few iterations, the method converges towards essentially the same predicted values, regardless of the initial guess for α_1 and T_0. Although the differences between the generated solutions were small, those with lowest Mean Least Square Error (MLSE) were chosen.

Table 3 exhibits the resulting parameter estimates for both tests. The ground conductivity estimates of 2.30W/m K and 2.36W/m K for tests $O1T1$ and $O1$ $T2$ respectively agree well with previous results. Also, grout conductivity parameter estimates of 0.70W/m K and 0.64W/m K are well in agreement and indicate that the chosen grout acts quite poorly in terms of performance. These values reflect not only the material grout conductivity as such, but also the combination of uncertainties (in the distances, etc.), or effects not taken into account in the model (such as short-circuiting between the U legs and heat resistances not accounted for) that limit heat conduction in our BHE.

In essence, the estimates obtained represent plausible values that may be close to but shall not be confused with a direct measurement of ground or grout properties, as C2RLS model represents an idealization of the physical system.

Interestingly, the different estimates for the diffusivity of soil and grout also agree quite closely and, from the data, we learn that, between α_1 and α_2, there is a substantial difference as grout diffusivity turns out to be approximately one fifth to one seventh of ground diffusivity, due to the combined effect of a lower conductivity and higher heat capacity of the backfill products. Indeed, the estimate for the diffusivities of ground and grout regions allow to deduce some values for the heat capacities in both regions. In the case of the ground, the volumetric heat capacity is estimated between 8×10^5 J/(K m^3) and 9.4×10^5 J/(K m^3), in good correspondence with the plausible estimates discussed in Appendix A.5.2. The backfill volumetric heat capacities are estimated in the range between 1.8×10^6 J/(K m^3) and 3.5×10^6 J/(K m^3) with matches with values known from cement samples.

Additionally, a way to estimate the borehole resistance is now available without being influenced by an improper guess of T_0 and α_1 using the obtained values found for the undisturbed ground temperature (T_0 = 20.65 °C). It is to mention here that in [27], a value of R_b = 0.2 m K/W was suggested in this context, but as previously discussed, this estimation depends substantially on the assumed values for T_0 and α. In the mentioned work T_0 = 20.12 °C and $\alpha = 0.6\times10^{-7}$ m^2/s are considered respectively in view of the information at hand. In contrast, this present analysis find notably higher values for the ground diffusivity and a somewhat higher undisturbed ground temperature. The observed difference in the R_b estimation can be exactly justified by employing Eq. (8), for if, instead of the diffusivity and undisturbed ground temperature given by the parameter estimation, using the alternative values assumed in [27], the borehole resistance value of 0.2 is recovered. From this analysis, we can conclude that, even if proper TRT procedures are applied, many borehole resistance values found in literature may be far of reality due to the wrong estimation of the ground conductivity.

As a concluding remark, it is noteworthy to observe the discrepancy in the pipe resistance values (0.0815 m K/W and 0.104 m K/W, for O1 T1 and O1 T2 respectively). These results, obtained theoretically from Eq. (6), are due to the difference in the flow rates of both tests, causing a variation in their characteristic Nusselt numbers. Notably, this difference could explain as well the slight drop in borehole resistance between O1 T1 and O1 T2.

Comparison of model vs. data. With the parameter values obtained as explained in the previous paragraphs, Fig. 7 shows the comparison between the predicted and measured average temperature response ($\frac{T_{in}+T_{out}}{2}$) in the case of test O1 T2, see Table 2, consisting of a single steady 32 day long heat constant injection with a 1 day previous period of water circulation without injection. The data used for the fitting of the ILS and steady C2RLS parts of our parameter estimation method (see Section 4.3) are shown as a thick gray region. The data to fit the unsteady C2RLS model cover the entire dataset and the resulting prediction based on the adjusted parameters is depicted as a dashed curve. We observe that the model matches well both steady and unsteady data segments.

4.5. *N* 1, 3 *and* 5 *results*

Plausible parameter set estimation. Both test replicas in the N 1 show quite similar results, though in general parameter estimation results in the "N" sites carry greater uncertainty than tests at the "O" site. Replica N1 T2 shows a far better MLSE than N1 T1 possibly due to the quite substantial improvement in the test site control hardware and algorithm between 2018 and 2022. The former will be used as the basis for further analysis. With a ground conductivity of 2.42 results

agree well with the expected values from previous measurements and from the known ground properties. Again the λ_1 parameter estimate (0.84) is lower than would be expected in view of the fact that during the construction of the N 1 BHE thermally enhanced grout badges were used. Nevertheless this result is particularly interesting as a reference datum for test sites N 3 and 5, backfilled with the new products.

The estimates about diffusivity of ground and grout obtained from our TRT results are in fully within the range of expected values from grout samples, as discussed in Appendix A.5.2. The related volumetric heat capacities are about $2300\,10^{-6}$ kJ/(m^3 K) for the ground (also quite in the median of the values obtained by sampling, as discussed in Appendix A.5.2) and $3450\,10^{-6}$ kJ/(m^3 K) for the backfill. The lower backfill diffusivity is a combined effect of its lower conductivity and higher heat capacity.

The plausible estimates for λ_1 corresponding to N 3 and N 5 confirm higher effective conductivities for the new grouts produced within GEOCOND project in comparison with reference N 1. The grout conductivity results for the N 3, and N 5 boreholes obtained by parameter estimation do not match with the results obtained by sampling as shown in Table 2. Whilst the reason for this mismatch was discussed in the previous subsection, it is seen that, when compared to the reference grout N 1, the new products provide a substantially higher effective conductivity. Results also show differences between grout in N 3 an N 5, being the latter the more efficient grout.

Table 2 shows consistently high estimated values for the ground conductivity λ_2 in the case of N 3 and N 5. To ensure that no artifacts were introduced by the fitting algorithm, these estimates have been confirmed by independent simulations using the Earth Energy Designer software and direct ILS estimation. There is some indication that some groundwater flow effects could be present that would explain this results. In N 3 tests the estimated ground heat capacity is clearly higher compared to N 1 and the other tests, which can be attributed to an increased presence of water. Also it should be noted that, according to standard deviation values, uncertainty in the estimation of N 3 parameters is increased compared to other tests. This may as well point to some influence that affects the ability of the model to represent the real situation.

The reasons for this anomaly can only be hypothesized without further study and may be due to the complex hydrogeology of the area, with overlying clay and gravel layers, a high water table and continuous disturbance and irrigation water injections from surrounding and nearby fields. The boreholes are shallow, so that certain structures at depth, such as pipes or ditches, could alter the distribution of saturated water inhomogeneously, creating significant differences over short distances. On the other hand, works such as Sharqawy et al. [39] indicate that, in soils with the aforementioned characteristics, thermal conductivity is not only due to heat transmission by conduction, but that phenomena such as free convection can significantly alter the effective conduction values. This would indicate that the pure conduction model would not be sufficient to describe the situation, but at the C2RLS level (which is a pure conduction model) it could manifest itself in the existence of estimated values that cannot be explained by the physical conditions of the soil.

In connection with borehole resistances, the interpretation of the TRT results by means of parameter estimation scheme shows that it was possible to step down R_b from about 0.126 of a standard BHE to 0.106 in the case N 5 with only the improved grouting and standard pipe. The use of the improved pipe in combination with the improved grout in the case of N 3 does not show up as a further reduction in the value of R_b but one must be cautious, for, as we have seen, the grout does not show the same efficiency and furthermore the uncertainty associated with N 3 data is markedly higher compared to the N5 T2 replica. This uncertainty could mask the effect of the improved pipe heat resistance in the value of the borehole resistance.

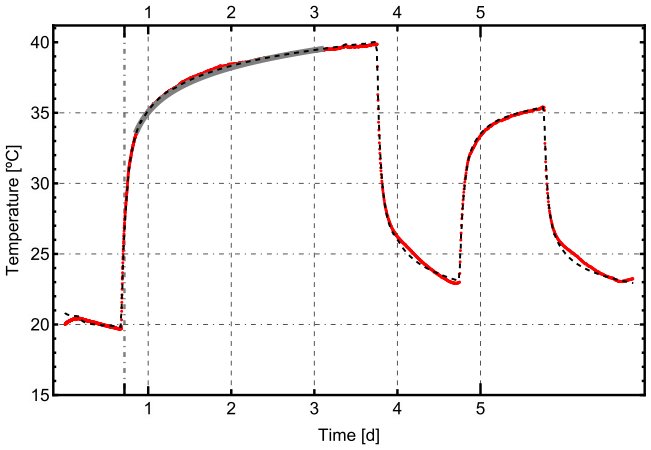

Fig. 8. Results of the data adjustment of the N 5 borehole experiment in the linear time domain. The dashed line corresponds to C2RLS unsteady model, gray curve shows the segment fitted with the ILS model, and TRT data (average temperature in the borehole) is shown in red.

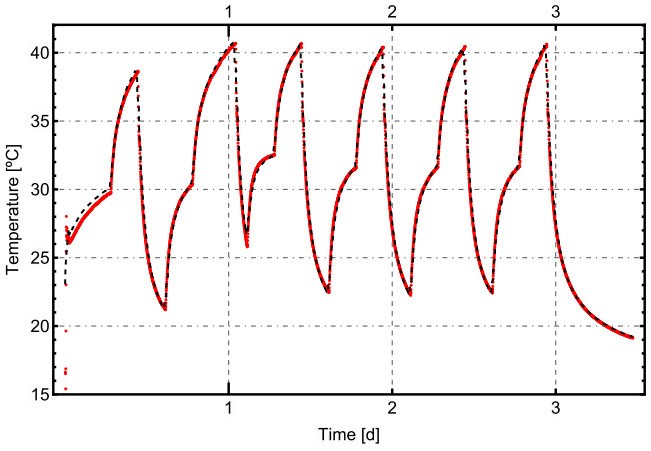

Fig. 9. Predicted versus measured temperatures using the estimated parameters of the N5 T2 and the N5 T3 measured heat injection rates to predict the temperature evolution. The dashed line corresponds C2RLS unsteady model and the TRT data (average temperature in the borehole) is shown in red.

Comparison of predicted responses vs. data. To produce Figs. 8 and 9, the estimated parameters to evaluate are used, in combination with the unsteady C2RLS model (10) and the discretized heat injection information, the BHE response to heat injection experiments different of those that were used for their estimation (such as N5 T3, which includes 6 on–off heating cycles). The parameters used to compute the predictions of the model in Fig. 9 are those extracted from the best fit of N5 T2 (performed some months afterwards).

The results of the rest of TRTs on boreholes N 1 and N 3 show similar trends between the predicted and measured responses as depicted in Fig. 8. The corresponding graphs are not shown here for the sake of compactness. These results provide a solid evidence of the ability of (10), together with the described parameter estimation method, to model dynamic response of real BHEs.

5. Conclusions and further outlook

A methodology has been developed that combines different existing TRT analysis methods, the infinite line and composite 2-region line source approaches (C2RLS), to estimate plausible values for soil and backfill parameters of thermal properties.

To this, C2RLS method has been adapted by calculating transfer functions that allow a reliable and reasonably efficient calculation. Besides, to improve the ability of the C2RLS model to obtain unambiguous parameters, a combination of steady and non-steady TRT data is proposed.

The values obtained by means of this approach posses distinctive features:

- Parameters otherwise difficult to obtain such as the diffusivities, heat capacities and conductivities of ground and grout and the pipe heat resistance are estimated, offering additional information for further improvements, its characterization and verification.
- All of them are correlated to actual physical, mensurable soil and ground properties, which allows independent critical revision and check against alternative estimation methods. Ground diffusivity and undisturbed ground temperature are amongst the estimated parameter. There is no need to rely on some previous independent estimation about their values.
- The estimated parameters provide a model that accurately allows to predict the non-stationary temperature evolution of a BHE, subject to any given non-steady heat injection sequence, as shown in Fig. 9.

The application of this methodology to 4 different boreholes offers additional information and insight about the characteristics of the materials developed within project GEOCOND and new lines of thought about future improvements of the standard TRT evaluation methods.

Additionally, the effect of the different materials in the overall borehole performance were characterized, and the improvements of the effective grout conductivity parameters were experimentally verified showing a considerable increase in the effective grout conductivity parameter and a reduced borehole resistance. The higher conductivity of the pipe material developed throughout the GEOCOND project also shows a marginal but positive influence on the BHE's performance.

The model is easily extensible to any configuration based on centered or off-centered pipes in any arrangement. This includes coaxial, single and double-U and our so-called trilobular configuration (based on an upflow central pipe and three satellite downward pipes).

As a future outlook, this work opens new avenues in different areas: from improving the standards for TRT analysis protocols, to the deepening in the search of solutions for a better utilization of the ground in borehole heat exchanger applications.

CRediT authorship contribution statement

Javier F. Urchueguía: Conceptualization, Model development, Formal analysis, Validation, Writing – original draft, Writing – review & editing, Supervision, Funding acquisition. **Borja Badenes:** Methodology, Investigation, Validation, Writing – original draft, Writing – review and editing. **Hossein Javadi:** Formal analysis, Writing – original draft, Writing – review & editing. **Miguel Ángel Mateo:** Formal analysis, Software, Visualization, Writing – original draft, Writing – review & editing. **Bruno Armengot:** Resources, Writing – original draft, Writing – review & editing.

Declaration of competing interest

The authors declare the following financial interests/personal relationships which may be considered as potential competing interests: Javier F. Urchueguia reports financial support was provided by European Union Horizon 2020 Research and Innovation program. Javier F. Urchueguia has patent Piping for adapted thermal conductivity pending to EP22382747.7.

Data availability

Data will be made available on request.

Acknowledgment

The authors are deeply indebted with the many colleagues who have, in one way or another, contributed to this research. We would like to specially acknowledge the fruitful discussions with Burkhard Sanner in the context of the TRT results and the many friends and collaborators in research projects CHEAP-GSHP, GEOCOND and GEO4CIVHIC that in many forms have been crucial in this endeavour.

Acknowledgment to GEO4CIVHIC:

This work has received funding from the European Union's Horizon 2020 Research and Innovation program under grant agreement No [792355].

Acknowledgment to the support from the Program for the Requalification of the Spanish university system for 2021–2023 (in the framework of the call of the Universitat Politècnica de València), subsidized by the European Recovery Instrument (financed by the European Union by Next Generation EU) in the framework of the Spanish Recovery, Transformation and Resilience Plan, through the Ministry of Universities, regulated by RD 289/2021 and Order UNI/551/2021.

Abbreviations and mathematical symbols

The following nomenclature and abbreviations are used in this manuscript:

BHE	Borehole Heat Exchanger
C2RLS	Composite 2-Region Line Source Model
CLS	Cylinder Line Source Model
FLS	Finite Line Source Model
GSHP	Ground Source Heat Pump
HDPE	High-density polyethylene
ILS	Infinite Line Source Model
MFLS	Moving Finite Line Source Model
MLSE	Mean Least Square Error
PB	Polybutylene
PCM	Phase Changing Materials
PID	Proportional–Integral–Derivative controller
PE-pipe	Polyethylene pipe
PEX	Cross-linked polyethylene
SGE	Shallow Geothermal Energy
TRT	Thermal Response Test
UPV	Universitat Politècnica de València
VDI	Verein Deutscher Ingenieure (English: Association of German Engineers)

Mathematical symbols are explained in the text.

Disclaimer

The information and views set out in this article are those of the authors and do not necessarily reflect the official opinion of the European Union. Neither the European Union institutions and bodies nor any person acting on their behalf may be held responsible for the use which may be made of the information contained therein.

Appendix A. Composite two-region line source model (c2rls) and its numerical implementation

A.1. Outline of the C2RLS model

For our analysis, the order and notation in [40] is followed. The basic solution used in this work developed by Jaeger [32], is the infinite instant line-source solution in composite cylindrical media.

We consider an infinite solid region composed of two cylindrical subregions, represented in cylinder coordinates with $r < r_b$ for the inner medium and $r > r_b$ for the outer. There is an infinite line-source of heat injection linear density equal to $\dot{q}_L$ instantly releasing heat into the solid composite starting at time zero.

The heat source is parallel to the z-axis and passes through a point (r', θ') in the $z = 0$ plane, while the point where the temperatures are observed/calculated is given by (r, θ). For the expressions to be calculated we will use the non-dimensional quantities $R = \frac{r}{r_b}$ and $R' = \frac{r'}{r_b}$ that correspond to the observation point distance, r and the center of the linear source, r'.

To relate more easily to g-functions, it is also convenient to express the temperature response in non-dimensional terms as $\Theta_i = \frac{2\pi\lambda_i T_i}{\dot{q}_L}$, where the sub index i is equal to 1 for the temperature response in the inner region ($R \leq 1$), while sub-index 2 corresponds to the response outside the core region ($R > 1$).

It is found that the temperature response is only function of three non-dimensional quantities. The first relates to time and is the Fourier number related to the borehole radius. In region 1 it is given by $\mathrm{Fo} = \alpha_1 \frac{t}{r_b^2}$, where α_1 is the ground diffusivity in region 1.

Furthermore two additional dimensionless quantities will play and important role. $k = \frac{\lambda_2}{\lambda_1}$ is the ratio of grout to ground conductivity, while a second parameter related to the ratio of grout/ground diffusivity given by $a = \sqrt{\frac{\alpha_1}{\alpha_2}}$ appears in the model.

For convenience, the a parameter has been substituted as originally shown in [32,40] with a further dimensionless quantity related to the ratio of volumetric heat capacities of ground and grout defined by:

$$\phi = \frac{cv_2}{cv_1}$$

If we consider that:

$$\alpha_i = \frac{\lambda_i}{cv_i} \qquad i = 1, 2,$$

then:

$$a = \sqrt{\frac{\lambda_1}{\lambda_2}\frac{cv_2}{cv_1}} = \sqrt{\frac{\phi}{k}}$$

The use of ϕ facilitates the analysis of results considering that k and ϕ are basically unrelated properties, while there is a strong relationship between k and a.

By means of the Laplace transform method, the heat equation and specific boundary conditions can be expressed explicitly and an analytic solution for the heat step can be found. Following equations (4a) and (4b) in [40], the temperature response of the above system in dimensionless terms by means of the following equations valid if $r' < r_b$:

$$\Theta_{l,1}(Fo, R, \theta) = \sum_{n=-\infty}^{+\infty} \cos n(\theta - \theta') \times \int_0^{+\infty} (1 - e^{-\upsilon^2 Fo}) \frac{J_n(\upsilon R) J_n(\upsilon R')(\varphi_n g_n - \psi_n f_n)}{\upsilon(\varphi_n^2 + \psi_n^2)} d\upsilon \tag{A.1}$$

$$\Theta_{2,1}(Fo, R, \theta) = \frac{2}{\pi} \sum_{n=-\infty}^{+\infty} \cos n(\theta - \theta') \times \int_0^{+\infty} (1 - e^{-\upsilon^2 Fo}) \frac{J_n(\upsilon R')(J_n(a\upsilon R)\psi_n - Y_n(a\upsilon R)\varphi_n)}{\upsilon^2(\varphi_n^2 + \psi_n^2)} d\upsilon, \tag{A.2}$$

where $n \in \mathbb{Z}$.

For TRT analysis, we are interested in region 1, as only information about temperatures right beneath the BHE wall is needed.

The functions appearing inside the integral are derivatives of products of Bessel functions and are given by the following expressions (for the sake of brevity $a = a(k, \phi)$ parameter has been kept in the expressions for the functions):

$$\varphi_n(\upsilon, \phi, k) = akJ_n(\upsilon)J_n'(ak\upsilon) - J_n'(\upsilon)J_n(a\upsilon)$$
$$\psi_n(\upsilon, \phi, k) = akJ_n(\upsilon)Y_n'(ak\upsilon) - Y_n'(\upsilon)J_n(a\upsilon)$$
$$f_n(\upsilon, \phi, k) = akY_n(\upsilon)J_n'(ak\upsilon) - J_n'(\upsilon)Y_n(a\upsilon)$$
$$g_n(\upsilon, \phi, k) = akY_n(\upsilon)Y_n'(ak\upsilon) - Y_n'(\upsilon)Y_n(a\upsilon),$$

being Jn and Y_n the Bessel functions of first and second kind and J_n' and Y_n' their first derivatives with respect to υ.

A.2. Single-u C2RLS g-function

In the adaptation of this method to TRT analysis by [40], the U tube BHE is represented by the superposition of two linear sources located which center is located at cylinder coordinates $(r_c, 0)$ and (r_c, π). The non dimensional temperature response is given as the average of the response at two locations placed in front and in the rear of the pipe. If r_p is the pipe radius, then, the coordinates of the two observation points in front of the first pipe are: $(r_c + r_p, 0)$ and $(r_c - r_p, 0)$, for one pipe and $(r_c + r_p, \pi)$ and $(r_c - r_p, \pi)$ for the second.

In terms of non dimensional quantities, the observation point coordinates can be related to the non dimensional shank spacing ($\eta = r_c/r_b$) and the non dimensional pipe radius ($\rho_p = r_p/r_b$). Moreover, $\eta \geq \rho_p$ for solutions is imposed to be feasible.

With these assumption and following the above notation, the g-function of a single U heat exchanger is computed as:

$$\begin{aligned} g_{su}(Fo, \eta, \rho_p, k, \phi) &= \frac{1}{2}((\Theta_{l,1}(Fo, \eta + \rho_p, 0) + \Theta_{l,1}(Fo, \eta + \rho_p, \pi)) + \\ &+ (\Theta_{l,1}(Fo, \eta - \rho_p, 0) + \Theta_{l,1}(Fo, \eta - \rho_p, \pi))) \\ &= \sum_{n=-\infty}^{+\infty} \cos n(\theta - \theta') \mathrm{K}_n(Fo, d, \eta, k, \phi). \end{aligned}$$

Taking into account that $\cos n\pi = (-1)^n$, only terms with even n in eq.(A.1) contribute to the g-function. Furthermore, the parity of the integrand in Eq. (A.1) is even if $n \to -n$, hence, after simplification we arrive at our final expression which states that:

$$g_{su}(Fo, d, \eta, k, \phi) = \sum_{n=0}^{+\infty} \mathrm{K}_{2n}(Fo, \eta, \rho_p, k, \phi), \tag{A.3}$$

where the function K_{2n} is given by:

$$\begin{aligned} \mathrm{K}_{2n}(Fo, \eta, \rho_p, k, \phi) &= \int_0^{+\infty} (1 - e^{-\upsilon^2 Fo}) \times \\ &\frac{2kJ_{2n}(\upsilon\rho_p)(J_{2n}(\upsilon(\eta - \rho_p)) + J_{2n}(\upsilon(\eta + \rho_p)))}{\pi^2\upsilon\left(\mathbb{A}_{2n}^2 + \mathbb{B}_{2n}^2\right)} d\upsilon \\ &\equiv \int_0^{+\infty} (1 - e^{-\upsilon^2 Fo}) F_{2n} d\upsilon, \end{aligned} \tag{A.4}$$

and where,

$$\mathbb{A}_{2n} = (ak\upsilon J_{2n}(\upsilon)J_{2n-1}(a\upsilon) - J_{2n}(a\upsilon)((k-1)2nJ_{2n}(\upsilon) + \upsilon J_{2n-1}(\upsilon)))$$
$$\mathbb{B}_{2n} = (J_{2n}(\upsilon)((k-1)2nY_{2n}(a\upsilon) - ak\upsilon Y_{2n-1}(a\upsilon)) + \upsilon J_{2n-1}(\upsilon)Y_{2n}(a\upsilon))$$

A.3. ILS as a special limit of the C2RLS

If the observation point location is set at $R = 1$ and the shank spacing is set to zero, we get the special case:

$$F_{2n} = \begin{cases} \frac{4kJ_0(\nu)}{\pi^2\nu^3\left(\mathbb{A}_0^2 + \mathbb{B}_0^2\right)} & n = 0 \\ 0 & n > 0 \end{cases} \tag{A.5}$$

In this situation, if furthermore the medium is homogeneous ($k = a = 1$), the calculation simply reduces to:

$$F_{2n} = \begin{cases} \frac{J_0(\upsilon)}{\upsilon} & n = 0 \\ 0 & n > 0 \end{cases} \tag{A.6}$$

Eq. (4) can be then integrated with the result:

$$g_{su_{lim}}(Fo, 0, 1, 1, 1) = \mathrm{K}_0(Fo, 0, 1, 1, 1) = \int_0^{+\infty} (1 - e^{-\upsilon^2 Fo}) \frac{J_0(\upsilon)}{\upsilon} d\upsilon = \frac{1}{2} \Gamma\left(0, \frac{1}{4\, Fo}\right), \tag{A.7}$$

where Γ is the incomplete Euler Gamma function. This result is also valid for small values of time and can be compared to the ILS solution. Indeed, if a series expansion is performed around large values of the Fourier number, we get:

$$g_{su_{lim}}(Fo, 0, 1, 1, 1) \approx \frac{1}{2}(\log(4\ Fo) - \gamma) + \frac{1}{8\ Fo} + O\left(Fo^{-2}\right), \tag{A.8}$$

in which the first two terms correspond to the time dependent part of the ILS g-function. On the other hand, (A.5) allows to extend the ILS model to a centered infinite linear source in a composite medium.

As concluding remark, we can see that the ILS model is a special limit of the C2RLS framework.

A.4. Numerical computation of the C2RLS g-function

Eq. (A.3) can be approximated numerically, but is computationally much slower and complicated to obtain than simple analytic expressions such as (1). To alleviate this shortcoming, our strategy is to construct, by means of spline interpolation, a multidimensional surrogate g-function - $\tilde{g}$ - close enough to the exact numerical g-function given by (A.3). To this aim, the exact function must be calculated in certain number of sampling points within a region of interest in the $(Fo, k, \phi, \eta, \rho_p)$ parameter space.

For a sufficiently large value of M, in each of the sampling points, the value of the exact g-function can be in practice approximated by means of the finite series:

$$g_{su_{i,j,k,l,s}} = g_{su}(Fo_i, k_j, \phi_k, \eta_l, \rho_{p_s}) = \sum_{n=0}^{M} \mathrm{K}_{2n}(Fo_i, k_j, \phi_k, \eta_l, \rho_{p_s}) = \sum_{n=0}^{M} \mathrm{K}_{2n;i,j,k,l,s} \tag{A.9}$$

in a sufficiently dense grid of $(Fo_i, k_j, \phi_k, \eta_l, \rho_{p_s})$ values.

The value of each $\mathrm{K}_{2n;i,j,k,l,s}$ is computed using numerical integration by means of the Gauß– Kronrod rule, which in this case was found to be the most efficient quadrature method. The corresponding function was programmed in Wolfram language, using version 13.0 of the Mathematica software package, by means of the *NIntegrate* function [48].

As convergence criterion, for each of the sample points to be computed, new terms were added to the series unless, for a given value M:

$$K_{2(M+1)} \leq \epsilon,$$

where ϵ is a prescribed accuracy threshold. In practice, good results are found if choosing $\epsilon = 10^{-5}$.

In a high-end personal computer (Intel Core i9 - 16 core processors and 64GB RAM) it took between 0.3 and 1.5 s to obtain each value of (A.3). To cover the parameter space sufficiently, we chose to calculate about 70.000 function values within the chosen parameter domain.

Finally, to construct the surrogate g-function from the pre-calculated table a SPLINE based interpolation is applied. The estimated g-functions works around 100 to 1000 times faster than the original function and, by random sampling, it is ensured that the results are accurate within the pre-established domain.

Once the function is calculated, it represents any possible BHE geometry and parameter configuration within the prescribed parameter space. Indeed, the same function is employed for the analysis of the four different BHEs considered in this study.

Currently, the computation of the C2RLS model requires substantially longer than the usual ILS model. The time required on a typical workstation based on a i9 processor with Wolfram Mathematica version 13.2 is of between 30 min and several hours using each of the cores for a different starting value of the grout diffusivity. For comparison, ILS requires less than a minute, typically. The basic factor that influences the computation time is the amount of data (based on TRT duration and sampling frequency) and the number of bins into which the heat injection timeline is split. Essentially, the more bins, the more precise is the adjustment, up to a limit. It was not the aim of this work to optimize computation time, but just to evaluate the feasibility of the approach. This is left as a future line of work.

A.5. Surrogate g-function parameter domain

The set of $\left\{ Fo_i, k_j, \phi_k, \eta_l, \rho_{p_s} \right\}$ is to be chosen in a way that any possible geometrical single U configuration and potential k and ϕ ground/grout parameter ratios would be covered.

A.5.1. Logarithmic time sampling

As that the change in the value of the g-function is much faster at smaller times, it is important, in order to capture the evolution of the function properly, to sample more densely at low Fourier numbers and less densely at higher values of *Fo*. One way of realizing this is to use a constant sample density in the logarithmic Fourier number scale.

For our computation, 5 sample points have been chosen in each Fourier number decade, in the interval $Fo \in (0.0001, \ldots, 1000)$, which covers sufficiently the time scales of a typical TRT experiment.

A.5.2. Expected values for the ground and backfill thermal properties as boundaries for the k and ϕ parameters

From expected values of soil parameters (conductivity, density and specific heat capacity) limits can be estimated to obtain a feasible parameter space and to judge whether a given solution obtained numerically is realistic or even feasible.

Regarding the estimations for $k = \lambda_2/\lambda_1$, we know from previous results,[27], that soil conductivity is close to 2.4 W/(mK) and from sample data, grout conductivity are expected within 0.9 W/(mK) (low conductivity grout) to 2.6 W/(mK) (high conductivity grout). Hence, k to be within $k = 1.4^{+0.8}_{-0.6}$ is expected.

In the case of N 1 BHE there is a precise description of the lithological column recorded during drilling with estimation of the volumetric heat capacities and conductivities and diffusivities of the different layers according to tests performed on a group of samples. This investigation was performed with the collaboration of the Spanish Geological Institute in the context of the Spanish project PITERM. According to the obtained records, the plausible intervals for the volumetric heat capacities would range between 700 kJ/(m^{3}K) and 3340 kJ/(m^{3}K) were the median value for each of the layers was estimated to be within 1600 kJ/(m^{3}K) and 2400 kJ/(m^{3}K). This boundary could also be used in the case of the rest of boreholes in this project, as lithologically the ground is similar. The corresponding ground diffusivity values are expected to be found within the interval 0.2×10^{-6} m^2/s and 1.9×10^{-6} m^2/s.

In absence of such specific information it is possible to refer to data found in literature, see [49–51]. It is important to note that there is a substantial difference between wet and dry soil heat capacities.

Regarding the density of backfills used, these were directly measured from samples obtained *in situ* during backfilling operation in NTS 1, 3 and 5, with values in the range 1850^{+250}_{-100} kg/m^3. Direct heat capacity measurements are not available and thus only estimates based

on grout composition can be made. From literature, we find the interval given by $(1.9 \pm 0.6) \times 10^6$ kJ/(m^{3}K) for certain type of grouts.

To calculate the surrogate g-functions, the ϕ-ratio parameter have been estimated to lie in the interval between 0.2 and 1.3 using different estimated scenarios.

Taking all these considerations together, the following restricted parameter domain is obtained as a feasible parameter domain for the computation of the surrogate $\tilde{\Theta}_{SU}$ function:

$$\mathbb{D} = \{0.001 \leq Fo \leq 1000, 0.3 \leq k \leq 4, 0.2 \leq \phi \leq 1.4, \} \quad \text{(A.10)}$$

A.6. Analysis of uncertainties

To obtain information about the uncertainties associated with the parameter estimations obtained, a large number of perturbed data sets from the original experimental data were created in [27] to investigate the sensitivity of the projected soil parameter values to experimental errors, either random or systematic. By adding an independent, normally distributed, random error to the actual experimental values of the inlet and outlet temperature and volume flow sensor readings — considering the temperature accuracy within ±0.1 K and a flow sensor accuracy of ±2%, each of these sets is created from the original observations.

This procedure allowed to dimension the uncertainty linked to sensor accuracy and random noise effects to be of 0.007 W/(m K) for the λ_2 parameter in the case of the "O" tests.

Evidently, other sources of errors may be present in this analysis. As is clear, there is an uncertainty in the estimation of the parameters λ_1, λ_2 and c_V that is connected both to its sensitivity within the nonlinear fitting procedure (as discussed in Section 4.1.2) and to the quality of the test in terms of noise and control. The plausibility intervals in this graph show approximately what could be the confidence region linked to the different parameters given the experimental situation. In our opinion, more tests and observations should be undertaken to arrive at definite conclusions in this regard.

Appendix B. Open data implementation

The data, algorithm, g-function coefficients and auxiliary files linked to this research will be shared as open-source material (data-in-brief under preparing). In the meantime, any data can be requested from the corresponding author upon request.

References

[1] J. Urchueguía, M. Zacarés, J. Corberán, Á. Montero, J. Martos, H. Witte, Comparison between the energy performance of a ground coupled water to water heat pump system and an air to water heat pump system for heating and cooling in typical conditions of the European Mediterranean coast, Energy Convers. Manage. 49 (10) (2008) 2917–2923, http://dx.doi.org/10.1016/j.enconman.2008.03.001.

[2] Advanced materials and processes to improve performance and cost-efficiency of shallow geothermal systems and underground thermal storage, 2017 – 2021, an European Union's Horizon 2020 project - GA No. 727583 (https://geocond-project.eu/- (Last accessed 22 July 2022)).

[3] H. Javadi, S.S. Mousavi Ajarostaghi, M.A. Rosen, M. Pourfallah, A comprehensive review of backfill materials and their effects on ground heat exchanger performance, Sustainability 10 (12) (2018) http://dx.doi.org/10.3390/su10124486.

[4] B. Badenes, B. Sanner, M.Á. Mateo Pla, J.M. Cuevas, F. Bartoli, F. Ciardelli, R.M. González, A.N. Ghafar, P. Fontana, L. Lemus Zuñiga, J.F. Urchueguía, Development of advanced materials guided by numerical simulations to improve performance and cost-efficiency of borehole heat exchangers (BHEs), Energy 201 (2020) 117628, http://dx.doi.org/10.1016/j.energy.2020.117628.

[5] Cheap and efficient application of reliable ground source heat exchangers and pumps, 2015 – 2019, an European Union's Horizon 2020 project - GA No. 657982 (https://cheaps-gshp.eu/ - (Last accessed 22 July 2022)).

[6] Most easy, efficient and low cost geothermal systems for retrofitting civil and historical buildings, 2018 – 2023, an European Union's Horizon 2020 project - GA No. 792355 (https://geo4civhic.eu/ - (Last accessed 22 July 2022)).

[7] H. Javadi, S.S. Mousavi Ajarostaghi, M.A. Rosen, M. Pourfallah, Performance of ground heat exchangers: A comprehensive review of recent advances, Energy 178 (2019) 207–233, http://dx.doi.org/10.1016/j.energy.2019.04.094.

[8] N. Batini, A.F. Rotta Loria, P. Conti, D. Testi, W. Grassi, L. Laloui, Energy and geotechnical behaviour of energy piles for different design solutions, Appl. Therm. Eng. 86 (2015) 199–213, http://dx.doi.org/10.1016/j.applthermaleng.2015.04.050.

[9] A. Carotenuto, P. Marotta, N. Massarotti, A. Mauro, G. Normino, Energy piles for ground source heat pump applications: Comparison of heat transfer performance for different design and operating parameters, Appl. Therm. Eng. 124 (2017) 1492–1504, http://dx.doi.org/10.1016/j.applthermaleng.2017.06.038.

[10] B. Badenes, T. Magraner, C. de Santiago, F. Pardo de Santayana, J.F. Urchueguía, Thermal behaviour under service loads of a thermo-active precast pile, Energies 10 (9) (2017).

[11] S. Gehlin, Thermal response test. In situ measurements for thermal properties in hard rock (Ph.D. thesis), University of Lulea, Sweden, 1998.

[12] B. Sanner, G. Hellström, J.D. Spitler, S. Gehlin, More than 15 years of mobile Thermal Response Test – a summary of experiences and prospects, in: Proceedings of the European Geothermal Congress 2013, 2013.

[13] A. Franco, P. Conti, Clearing a path for ground heat exchange systems: A review on thermal response test (TRT) methods and a geotechnical routine test for estimating soil thermal properties, Energies 13 (2020) 2965.

[14] H.J.L. Witte, G.J. Van Gelder, J.D. Spitier, In situ measurement of ground thermal conductivity: a Dutch perspective, Ashrae Trans. 108 (2002) 263.

[15] W. Austin, C. Yazuzturk, J. Spitler, Development of an in-situ system and analysis procedure for measuring ground thermal properties, Ashrae Trans. 106 (1) (2000).

[16] J. Shonder, J. Beck, Field test of a new method for determining soil formation thermal conductivity and borehole resistance, in: Ashrae Transactions, 2000.

[17] P. Eskilson, Thermal Analysis of Heat Extraction Boreholes (Ph.D. thesis), Grahns Boktryckeri AB, Lund University, 1987, p. 222, URL http://www.buildingphysics.com/Eskilson1987.pdf.

[18] L. Lamarche, B. Beauchamp, A new contribution to the finite line-source model for geothermal boreholes, Energy Build. 39 (2) (2007) 188–198, http://dx.doi.org/10.1016/j.enbuild.2006.06.003, URL http://www.sciencedirect.com/science/article/pii/S0378778806001824.

[19] T.V. Bandos, Á. Montero, E. Fernández, J.L.G. Santander, J.M. Isidro, J. Pérez, P.J.F. de Córdoba, J.F. Urchueguía, Finite line-source model for borehole heat exchangers: effect of vertical temperature variations, Geothermics 38 (2) (2009) 263–270, http://dx.doi.org/10.1016/j.geothermics.2009.01.003.

[20] N. Molina-Giraldo, Heat transport modeling in shallow aquifers (Ph.D. thesis), Mathematisch-Naturwissenschaftlichen Fakultät der Eberhard Karls Universität Tübingen, 2011.

[21] T. Magraner, Á. Montero, A. Cazorla-Marín, C. Montagud-Montalvá, J. Martos, Thermal response test analysis for U-pipe vertical borehole heat exchangers under groundwater flow conditions, Renew. Energy 165 (2021) 391–404, http://dx.doi.org/10.1016/j.renene.2020.11.029.

[22] M.D. Carli, M. Tonon, A. Zarrella, R. Zecchin, A computational capacity resistance model (CaRM) for vertical ground-coupled heat exchangers, Renew. Energy 35 (7) (2010) 1537–1550, http://dx.doi.org/10.1016/j.renene.2009.11.034, Special Section: IST National Conference 2009.

[23] A. Cazorla-Marín, C. Montagud-Montalvá, J.M. Corberán, Á. Montero, T. Magraner, A TRNSYS assisting tool for the estimation of ground thermal properties applied to TRT (thermal response test) data: B2G model, Appl. Therm. Eng. 185 (2021) 116370, http://dx.doi.org/10.1016/j.applthermaleng.2020.116370.

[24] B. Badenes, M. Mateo Pla, G.L. Lemus-Zúñiga, B. Sáiz Mauleón, J.F. Urchueguía, On the influence of operational and control parameters in thermal response testing of borehole heat exchangers, Energies 10 (9) (2017) http://dx.doi.org/10.3390/en10091328.

[25] H. Witte, A. van Gelder, Geothermal response tests using controlled multi-power level heating and cooling pulses (MPL–HCP), in: Proceedings of 10th International Conference on Thermal Energy Storage, Ecostock 2006, 2006.

[26] H.J. Witte, Error analysis of thermal response tests, Appl. Energy 109 (2013) 302–311, http://dx.doi.org/10.1016/j.apenergy.2012.11.060, URL http://www.sciencedirect.com/science/article/pii/S0306261912008653.

[27] J.F. Urchueguía, L.-G. Lemus-Zúñiga, J.-V. Oliver-Villanueva, B. Badenes, M.A. Mateo Pla, J.M. Cuevas, How reliable are standard thermal response tests? An assessment based on long-term thermal response tests under different operational conditions, Energies 11 (12) (2018) http://dx.doi.org/10.3390/en11123347.

[28] VDI 4640-2 (2016), Thermal use of the underground - Direct uses, Tech. rep., 2016.

[29] R.A. Beier, M.D. Smith, Minimum duration of in-situ tests on vertical boreholes, ASHRAE Trans 109 (2003).

[30] M. Li, A.C.K. Lai, Analytical model for short-time responses of ground heat exchangers with U-shaped tubes: Model development and validation, Appl. Energy 104 (2013) 510–516, http://dx.doi.org/10.1016/j.apenergy.2012.10.057.

[31] M. Li, A.C. Lai, Review of analytical models for heat transfer by vertical ground heat exchangers (GHEs): A perspective of time and space scales, Appl. Energy 151 (2015) 178–191, http://dx.doi.org/10.1016/j.apenergy.2015.04.070.

[32] H.S. Carslaw, J.C. Jaeger, Conduction of Heat in Solids, OXFORD UNIV PR, 1986.

[33] R.A. Beier, M.D. Smith, J.D. Spitler, Reference data sets for vertical borehole ground heat exchanger models and thermal response test analysis, Geothermics 40 (2011) 79–85, http://dx.doi.org/10.1016/j.geothermics.2010.12.007.

[34] M. Li, L. Zhang, G. Liu, Estimation of thermal properties of soil and backfilling material from thermal response tests (TRTs) for exploiting shallow geothermal energy: Sensitivity, identifiability, and uncertainty, Renew. Energy 132 (2019) 1263–1270, http://dx.doi.org/10.1016/j.renene.2018.09.022.
[35] B. Badenes, M.A. Mateo Pla, T. Magraner, J. Soriano, J.F. Urchueguía, Theoretical and experimental cost–benefit assessment of borehole heat exchangers (BHEs) according to working fluid flow rate, Energies 13 (18) (2020) http://dx.doi.org/10.3390/en13184925.
[36] P. Eskilson, J. Claesson, Simulation model for thermally interacting heat extraction boreholes, Numer. Heat Transfer 13 (2) (1988) 149–165, http://dx.doi.org/10.1080/10407788808913609.
[37] H. Zeng, N. Diao, Z. Fang, Heat transfer analysis of boreholes in vertical ground heat exchangers, Int. J. Heat Mass Transfer 46 (2003) 4467–4481.
[38] S. Signorelli, S. Bassetti, D. Pahud, T. Kolh, Numerical evaluation of thermal response tests, Geothermics 36 (2007) 141–166.
[39] M.H. Sharqawy, E.M. Mokheimer, H.M. Badr, Effective pipe-to-borehole thermal resistance for vertical ground heat exchangers, Geothermics 38 (2009) http://dx.doi.org/10.1016/j.geothermics.2009.02.001.
[40] M. Li, A.C.K. Lai, Parameter estimation of in-situ thermal response tests for borehole ground heat exchangers, Int. J. Heat Mass Transfer 55 (2012) http://dx.doi.org/10.1016/j.ijheatmasstransfer.2011.12.033.
[41] VDI Heat Atlas, Springer Berlin, Heidelberg, 2010.
[42] I.G. y Minero de España, Hydrogeological map of Spain, 2020, (last accessed 15 October 2020).
[43] D. Hillel, Fundamentals of soil physics, New York, 1982.
[44] J.M. Andújar Márquez, M.Á. Martínez Bohórquez, S. Gómez Melgar, Ground thermal diffusivity calculation by direct soil temperature measurement. Application to very low enthalpy geothermal energy systems, Sensors 16 (3) (2016) 306.
[45] M.A. Mateo Pla, B. Badenes, L. Lemus, J.F. Urchueguía, Assessing the shallow geothermal laboratory at universitat politècnica de valència, in: Proceedings of the European Geothermal Congress 2019, 2019.
[46] M. Ozisik, M. Orlande, Inverse Heat Transfer: Fundamentals and Applications, first ed., Taylor & Francis, New York, 1977.
[47] J. Beck, K. Arnold, Parameter Estimation in Engineering and Science, first ed., John Wiley & Sons, 1977.
[48] Wolfram Research, Inc., Mathematica 13.1, 2022.
[49] D. Kim, S. Oh, Relationship between the thermal properties and degree of saturation of cementitious grouts used in vertical borehole heat exchangers, Energy Build. 201 (2019) 1–9, http://dx.doi.org/10.1016/j.enbuild.2019.07.017.
[50] J. Poděbradská, J. Pavlík, J. Toman, R. Černý, Specific heat capacity of cementitious composites in high - temperature range, in: Proceedings of the Thermophysics 2003 Meeting of the Thermophysical Society Working Group of the Slovak Physical Society, 2003.
[51] Last accessed 30 september 2021, 2021, URL https://www.engineeringtoolbox.com/specific-heat-capacity-d_391.html.